

See discussions, stats, and author profiles for this publication at: <https://www.researchgate.net/publication/5531473>

Electron Permeable Self-Assembled Monolayers of Dithiolated Aromatic Scaffolds on Gold for Biosensor Applications

ARTICLE in ANALYTICAL CHEMISTRY · MAY 2008

Impact Factor: 5.64 · DOI: 10.1021/ac702195v · Source: PubMed

CITATIONS

60

READS

49

4 AUTHORS:



Alex Fragoso

Universitat Rovira i Virgili

93 PUBLICATIONS 1,744 CITATIONS

SEE PROFILE



Noemi Laboria

9 PUBLICATIONS 185 CITATIONS

SEE PROFILE



Daniel Latta

Institut für Mikrotechnik Mainz

18 PUBLICATIONS 216 CITATIONS

SEE PROFILE



Ciara Kathleen O'Sullivan

Universitat Rovira i Virgili

163 PUBLICATIONS 3,377 CITATIONS

SEE PROFILE

Electron Permeable Self-Assembled Monolayers of Dithiolated Aromatic Scaffolds on Gold for Biosensor Applications

Alex Fragoso,^{*,†} Noemi Laboria,[†] Daniel Latta,[‡] and Ciara K. O'Sullivan^{*,†,§}

Nanobiotechnology & Bioanalysis Group, Departament d'Enginyeria Química, Universitat Rovira i Virgili, Avinguda Paisos Catalans 26, 43007 Tarragona, Spain, Fluidics & Simulation, Institut für Mikrotechnik Mainz GmbH, Carl Zeiss Strasse 18-20, 55129 Mainz, Germany, and Institució Catalana de Recerca i Estudis Avançats, Passeig Lluís Companys, 23, 08010 Barcelona, Spain

Self-assembled monolayers (SAMs) of thiolated compounds are formed by the spontaneous chemisorption of thiolate groups on metal surfaces. In biosensors, they are most commonly used to covalently immobilize a biorecognition molecule onto the surface of the transducer, thus offering the possibility of controlling the orientation, distribution, and spacing of the sensing element while reducing nonspecific interactions. In this paper, self-assembled monolayers of dithiolated derivatives of 3,5-dihydroxybenzyl alcohol containing carboxyl and hydroxyl end groups have been prepared on gold surfaces and characterized by cyclic voltammetry and electrochemical impedance spectroscopy. Impedance measurements revealed that SAM formation is essentially completed after 3–5 h of exposure by observing the successive blocking of the faradic response of ferricyanide anion due to the adsorption of the dithiol molecules. The surface coverage of these molecules, estimated by reductive desorption experiments, was in the range of $(1.1–2.8) \times 10^{-10}$ mol/cm². To demonstrate the potential of the dithiol SAM, a model system for detection of a tumor marker, prostate-specific antigen (PSA), was developed. The carboxyl groups of the SAM were succinimide-activated, and an anti-PSA antibody was covalently immobilized via amide bonds. The modified SAM was used for the label-free detection of prostate-specific antigen using EIS with a detection limit of 9 ng/mL. The results described here demonstrate that this kind of dithiol-modified SAM can be used as supports in electrochemical biosensors and the results are explained in terms of the structural features of these dithiols.

Self-assembled monolayers (SAMs) of thiolated compounds are ordered structures formed by the chemisorption of thiolate groups on metal surfaces.¹ Gold has been the most extensive studied SAM support since it provides a stable and conductive surface and many optical, piezoelectric and electrochemical biosensors exploiting SAMs of gold have been reported.² In

biosensors, alkanethiol SAMs are most commonly used to covalently immobilize a biorecognition molecule (typically an enzyme, antibody, or nucleic acid sequence) onto the surface of the transducer since they offer the possibility of controlling the orientation, distribution, and spacing of the sensing element while reducing nonspecific interactions.³ However, while long-chain SAMs are very stable and effective in reducing/eliminating nonspecific binding,^{4,5} they have limited applicability in electrochemical biosensors since they show a low permeability to electron transfer, blocking the electrochemical response. This disadvantage could be circumvented with the use of alkanethiol mixtures having different chain lengths, but the low biomolecule immobilization capacity of these surfaces negatively influences the performance of the sensor.⁶

Recently, SAMs of dithiolated scaffolds **1–3** (Chart 1) have been studied as supports for the immobilization of antibodies and oligonucleotide probes.^{7–10} These molecules are derived from 3,5-dihydroxybenzyl alcohol and contain two identical alkylthiol substituents attached to the phenyl ring through phenolate bridges that provide two attachment points on the metallic surface (Figure 1). It can therefore be anticipated that these molecules will generate more stable SAMs than monothiols due to a multivalent mechanism of interaction and also provide a more adequate spacing of an immobilized biomolecule, thus allowing an improved mobility and flexibility at the recognition terminus.⁷ In addition, the benzylic core in **1** and **2** is modified with carboxyl group terminated alkyl chains onto which several types of biomolecules can be attached via amide bonds while **3** contains a poly(ethylene glycol) chain that can be used to prevent nonspecific interactions.⁵ This structure, with a dithiol anchor and a single tail, should have less insulating properties than alkylthiol SAMs and therefore are expected to be permeable to electron transfer, making these

* To whom correspondence should be addressed. E-mail: alex.fragoso@urv.cat; ciara.osullivan@urv.cat.

[†] Universitat Rovira i Virgili.

[‡] Institut für Mikrotechnik Mainz GmbH.

[§] Institució Catalana de Recerca i Estudis Avançats.

(1) Ulman, A. *Chem. Rev.* **1996**, *96*, 1533.

(2) Gooding, J. J.; Mearns, F.; Yang, W.; Liu, J. *Electroanalysis* **2003**, *15*, 81.

(3) Gooding, J. J.; Hibbert, D. B. *Trends Anal. Chem.* **1999**, *18*, 525.

(4) Ostuni, E.; Yan, L.; Whitesides, G. M. *Colloids Surf. B* **1999**, *15*, 3.

(5) Frederix, F.; Bonroy, K.; Reekmans, G.; Laureyn, W.; Campitelli, A.; Abramov, M. A.; Dehaen, W.; Maes, G. J. *Biochem. Biophys. Methods* **2004**, *58*, 67.

(6) Bonroy, K.; Frederix, F.; Reekmans, G.; Dewolf, E.; de Palma, R.; Borghs, G.; Declercq, P.; Goddeeris, B. J. *Immunol. Methods* **2006**, *312*, 167.

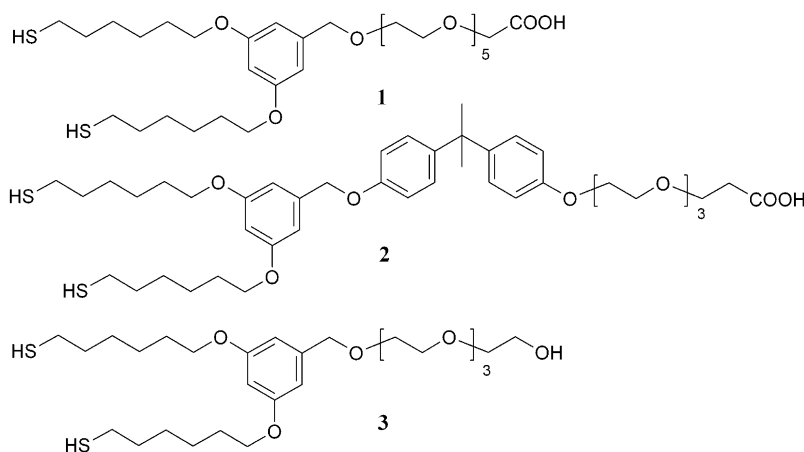
(7) Spangler, C. W.; Spangler, B. D.; Tarter, E. S.; Suo, Z. *Polym. Prepr.* **2004**, *45*, 524.

(8) Gobi, K. V.; Iwasaka, H.; Miura, N. *Biosens. Bioelectron.* **2007**, *22*, 1382.

(9) Nakamura, F.; Ito, E.; Hayashi, T.; Hara, M. *Colloids Surf. A* **2006**, *495*, 284–285.

(10) Subramanian, A.; Irudayaraj, J.; Ryan, T. *Sens. Actuators, B* **2006**, *114*, 192.

Chart 1. Dithiols Used in This Work



molecules attractive candidates for the construction of electrochemical biosensors.

The ability of these dithiol-modified SAMs to be exploited for biosensing has been mainly investigated by surface plasmon resonance (SPR). Label-free detection of insulin has been performed using an assay in which insulin was immobilized on a SAM of **1** and detected with nanomolar sensitivity by displacement of an insulin/anti-insulin complex.⁸ Additionally, the covalent attachment of a 30-mer ssDNA probe on SAMs of **1** and **2** and the qualitative detection of a model DNA target by SPR and X-ray photoelectron spectroscopy has been reported.⁹ Finally, an antibody-based detection of *Streptococcus aureus* on mixed SAMs of **1** and **3** has been developed with a detection limit of 10^5 cfu/mL and good specificity against *Escherichia coli*.¹⁰ To the best of our knowledge, no electrochemical characterization of SAMs of these dithiols has been reported in spite of the obvious advantages these dithiols offer in terms of SAM stability, versatility, reduction of nonspecific interactions, and application in electrochemical biosensors.

In this paper, we report the electrochemical properties of SAMs of dithiols **1** and **2** on gold and evaluate their application in

impedimetric immunosensors using prostate-specific antigen (PSA) as a model system. Electrochemical impedance spectroscopy (EIS) is a very useful technique for the characterization of surface phenomena that is increasingly finding applications in biosensing.¹¹ In comparison to amperometric detection, EIS assays are simpler, require fewer steps, and can provide direct immunosensing responses exploiting one-step capture formats obviating the need for sandwich-type designs using enzyme-labeled secondary probes, as required for amperometric immunosensors.

The model analyte, PSA, is a 30-kDa single-chain glycoprotein expressed predominantly by human prostate. It is usually present in the blood at low concentrations (<4 ng/mL) in healthy males, and because of the correlation of PSA concentration with tumor volume and tissue specificity, its use as a tumor marker for prostate cancer has flourished over the past decade.^{12,13} Electrochemical detection of PSA using biosensors has been carried out in the past by amperometry,^{14–16} but there are very few reports of impedimetric labelless electrochemical assays for PSA detection^{17–19}

EXPERIMENTAL SECTION

Materials. Dithiols **1–3** were purchased from SensoPath Technologies (Bozeman, MT) and used as received. The 1 mM stock solutions were prepared in absolute ethanol, purged with argon and kept at $-20\text{ }^{\circ}\text{C}$ when not used. Potassium hexacyanoferrate, *p*-aminophenol (pAP), 1-ethyl-3-(3-dimethylaminopropyl) carbodiimide hydrochloride (EDC), and *N*-hydroxysuccinimide (NHS) were purchased from Aldrich. PSA and carcinoembryonic antigen (CEA) were purchased from Scipac Ltd. Anti-PSA (PSA66) and anti-CEA (12-140-10) monoclonal antibodies were provided by Fujirebio Diagnostics AB and were used as received.

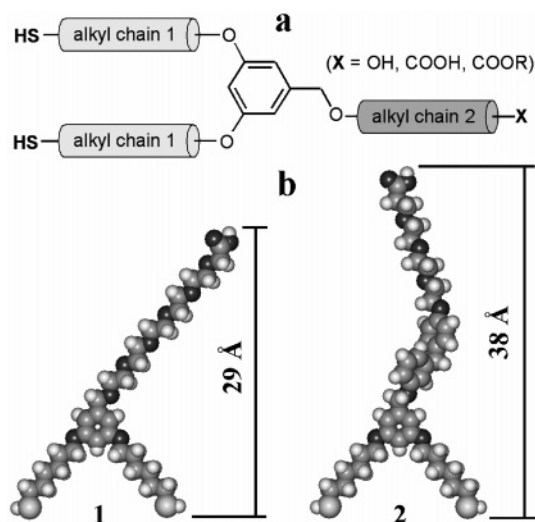
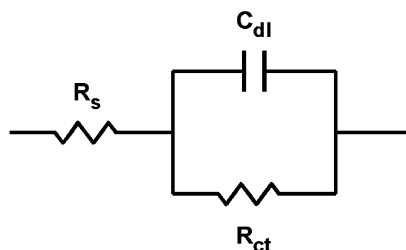


Figure 1. (a) Structural features of dithiols derived from 3,5-dihydroxybenzyl alcohol. (b) Energy minimized geometries and molecular dimensions of **1** and **2** (calculated using the semiempirical PM3 algorithm supported on HyperChem software, Version 7.0).

- (11) Daniels, J. S.; Pourmand, N. *Electroanalysis* **2007**, *19*, 1239.
- (12) Stenman, U.-H.; Leinonen, J.; Zhang, W.; Finne, P. *Semin. Cancer Biol.* **1999**, *9*, 83.
- (13) Healy, A.; Hayes, C. J.; Leonard, P.; McKenna, L.; O'Kennedy, R. *Trends Biotechnol.* **2007**, *25*, 125.
- (14) Zhang, S.; Dua, P.; Lia, F. *Talanta* **2007**, *72*, 1487.
- (15) Sarkar, P.; Pal, P. S.; Ghosh, D.; Setford, S. J.; Tothill, I. E. *Int. J. Pharm.* **2002**, *238*, 1.
- (16) Chen, S.-F.; Xu, Y.; Ip, M. P. *Clin. Chem.* **1997**, *43*, 1459.
- (17) Fernández-Sánchez, C.; Gallardo-Soto, A. M.; Rawson, K.; Nilsson, O.; McNeil, C. J. *Electrochem. Commun.* **2004**, *6*, 138.
- (18) Fernández-Sánchez, C.; McNeil, C. J.; Rawson, K.; Nilsson, O. *Anal. Chem.* **2004**, *76*, 5649.
- (19) Briman, M.; Artukovic, E.; Zhang, L.; Chi, D.; Goodglick, L.; Gruner, G. *Small* **2007**, *3*, 758.

Scheme 1. Equivalent Circuit Used to Model the Impedance Data (R_s , Solution Resistance; R_{ct} , Resistance to Charge Transfer; C_{dl} , Double Layer Capacitance)



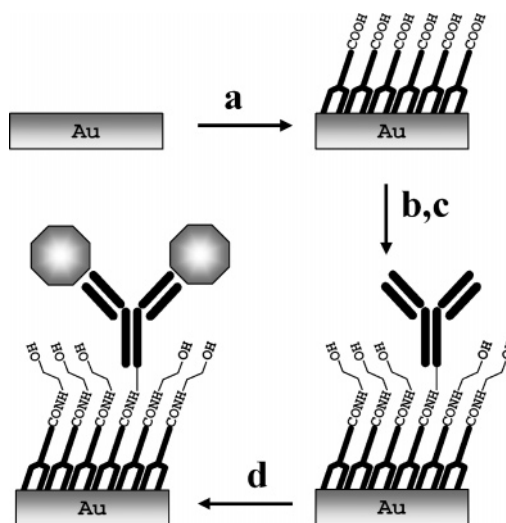
Electrochemical Instrumentation. Electrochemical measurements were performed on a PC controlled PGSTAT12 Autolab potentiostat (EcoChemie, The Netherlands) with an built-in frequency response analyzer FRA2 module. Electrochemical impedance measurements were performed using a standard three-electrode configuration (reference electrode, Ag/AgCl(sat.), counter electrode Pt wire) in 1 mM $\text{Fe}(\text{CN})_6^{3-/4-}$ in 0.1 M KCl. The impedance spectra were recorded over the frequency range of 10 kHz–0.1 Hz at a bias potential of +0.22 V and an ac amplitude of 5 mV. The impedance data were represented in the complex impedance plot (Nyquist plot), and the electrochemical parameters were obtained from simulation using the Autolab FRA software. The equivalent circuit used to model the impedance data is shown in Scheme 1.

Electrode Fabrication. Sputtered gold working electrodes were fabricated at the Institut für Mikrotechnik Mainz GmbH as follows. A silicon wafer was first insulated with a 150-nm layer of SiO_2 followed by an adhesive layer of 20-nm chromium. A 200-nm gold layer was then sputtered and structured by a liftoff process to shape an i.d. = 4 mm gold circle connected to a 10×8 mm contact pad through a 1-mm gold wire. The wafer was then insulated with a 5- μm layer of SU-8 photoresist leaving only exposed an i.d. = 3 mm circular working surface and the contact pad. The wafer was diced into 10×40 mm² pieces, and the electrode surface was cleaned in oxygen plasma (100 W, 5 min). This method allowed the preparation of several dozens of electrodes with a high degree of reproducibility (7.06 ± 0.01 mm²) of the electrode area.

Electrochemical Characterization of the SAMs. Immediately prior to use, the electrodes were cleaned again by three cycles of 10-min exposure to an ozone atmosphere using a PSD-UVT cleaning instrument (Novascan Technologies, Ames, IA), followed by rinsing with ethanol and drying in an argon stream. For the impedimetric study of SAM formation, the clean gold electrodes were modified by immersion in a freshly prepared 1 mM ethanol solution of **1** or **2** for fixed times followed by rinsing with copious amounts of ethanol and argon dried. These ethanol washings have been reported to effectively remove nonchemisorbed molecules as detected using a quartz crystal microbalance.^{9,10} After each modification and washing, faradic EIS and cyclic voltammetry (CV) were recorded using 1 mM $\text{Fe}(\text{CN})_6^{3-/4-}$ in 0.1 M KCl as an electroactive probe; the electrodes were then washed with Milli-Q water, argon dried, and immersed again in the modifying dithiol solution.

For the study of the acid–base properties of the SAMs, electrodes were modified with **1** (for 3 h) or **2** (for 5 h), followed

Scheme 2. Strategy for Electrode Modification and Antibody Immobilization (See Experimental Section for Details)



by rinsing with ethanol. The pH of 1 mM solution of $\text{K}_3\text{Fe}(\text{CN})_6$ in 0.1 M KCl was initially adjusted to 1.4 with 0.1 M HCl and the CV of the SAM-modified electrodes was recorded. The pH of the solution was then increased by addition of 0.1–1 M NaOH aliquots (also containing 1 mM $\text{K}_3\text{Fe}(\text{CN})_6$ and 0.1 M KCl in order to avoid dilution of the ferricyanide probe) and the CV was recorded again. The interfacial pK_a were then estimated from the inflection point of the peak current (at 0.39 V) versus pH plot (fitting the experimental points to a sigmoidal curve).

To test the electron-transfer properties, SAMs of **1** and **2** were prepared as described above and immersed in 0.1 M phosphate buffer pH 7. The background response in the potential range of –0.1–0.4 V was recorded using differential pulse voltammetry (DPV). The concentration of pAP (1–10 μM) was adjusted by adding aliquots of a 1 mM stock solution of pAP in Tris buffer pH 7.6 and the DPV response was recorded after every addition.

Nonspecific Binding Studies, Optimization of Antibody Immobilization and Antigen Detection Experiments. The gold electrodes were modified according to Scheme 2. Nonspecific binding was studied impedimetrically in two different ways: (i) recording the EIS before and after incubation of the corresponding SAM with 1 $\mu\text{g}/\text{mL}$ PSA for 5 min; (ii) clean gold electrodes were immersed in a 1 mM ethanolic solution of **1** for 3 h and washed with ethanol (Scheme 2a). The carboxyl groups of the SAM were sequentially modified by stirring the electrode in an aqueous mixture of EDC (0.2 M) and NHS (50 mM) for 30 min followed by immersion in a 0.1 mg/mL solution of anti-PSA or anti-CEA antibodies (PSA66 and 12-140-10, respectively, from Fujirebio Diagnostics AB) in acetate buffer pH 5 for 1 h with stirring (Scheme 2b). The remaining carboxyl groups were then blocked with 0.1 M ethanolamine hydrochloride (pH 8.5) for 30 min (Scheme 2c). EIS of the antibody-modified surface was recorded before and after incubation with 1 $\mu\text{g}/\text{mL}$ of the corresponding nonspecific antigen for 5 min using $\text{Fe}(\text{CN})_6^{3-/4-}$ as electroactive probe. The R_{ct} values were extracted from simulation of the complex impedance plot.

The specific recognition of PSA was optimized as follows. Ethanolic solutions having different **1** + **3** molar compositions

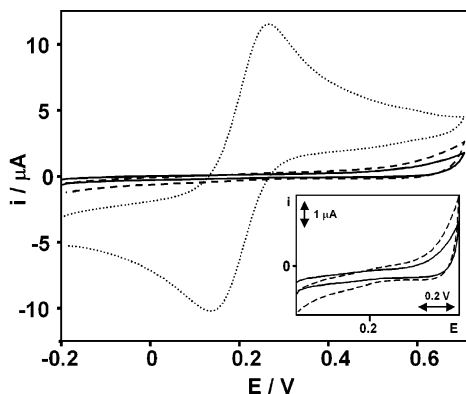


Figure 2. Cyclic voltammograms (in 1 mM $\text{K}_3\text{Fe}(\text{CN})_6$ in 0.1 M KCl) obtained at bare gold (dotted line), SAM of **1** (dashed line), and **2** (solid line).

(100:0, 50:50, 25:75, 5:95) were prepared to have a 1 mM total dithiol concentration. Clean gold electrodes were then immersed in these solutions for 3 h and washed with ethanol. PSA66 monoclonal antibody was then immobilized on these SAMs as described above followed by blocking with ethanolamine (Scheme 2a–c). The electrodes were then exposed to a $1 \mu\text{g}/\text{mL}$ solution of PSA for 5 min (Scheme 2d), followed by washing with 0.1 M Tris buffer pH 7.6 (containing 0.1% v/v Tween 20) to remove nonspecifically bound antigen, and EIS was recorded using $\text{Fe}(\text{CN})_6^{3-/4-}$ as electroactive probe.

For the impedimetric detection of PSA, a SAM composed of 100% **1** was formed and modified with anti-PSA antibody as described above (Scheme 2a–c). Stock solutions of PSA (from Scipac Ltd.) were prepared in 0.15 M NaCl and $20\text{-}\mu\text{L}$ aliquots of 1–1000 ng/mL were deposited on the modified electrodes and incubated for 5 min at room temperature (Scheme 2d). After washing with 0.1 M Tris buffer pH 7.6 (containing 0.1% v/v Tween 20) to remove nonspecifically bound antigen, EIS was recorded using $\text{Fe}(\text{CN})_6^{3-/4-}$ as electroactive probe.

RESULTS AND DISCUSSION

Formation and Characterization of SAMs. The process of SAM formation of dithiols **1** and **2** was monitored by CV and EIS. The CVs of the $\text{Fe}(\text{CN})_6^{3-/4-}$ redox couple at bare and SAM-modified electrodes were recorded, revealing the characteristic blocking effect on the CV response due to the formation of packed SAMs of **1** and **2** on the gold surfaces (Figure 2). Although both SAMs gave essentially the same qualitative result (a noticeable decrease in CV responses), it can be observed that the residual currents on the SAM of **2** are $\sim 40\%$ lower than those obtained with **1**, suggesting that **2** exerts a more pronounced barrier effect.

Figure 3 shows the impedance responses of SAMs of **1** and **2** in the presence of 1 mM $\text{Fe}(\text{CN})_6^{3-/4-}$ at different lengths of exposure time to the dithiol solution and the time dependence of the resistance to charge transfer obtained from simulation. The impedance values increased steadily with time until a constant value was obtained after several hours. This is indicative of the successive blocking of the surface by the adsorption of the dithiol molecules. In the presence of **1**, the impedance increase reached a maximum of 28 k Ω after 3 h, while SAMs of dithiol **2** needed up to 5 h and provoked a notable impedance increase (477 k Ω). These differences may be a consequence of the different nature

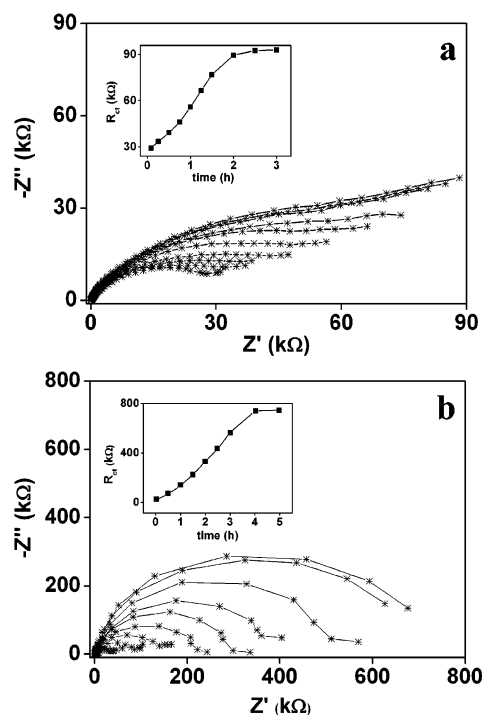


Figure 3. Complex impedance plots for the formation of SAMs of dithiols **1** (a) and **2** (b). The time dependence of R_{ct} values (obtained from simulation) are shown in the inset.

of the alkyl chain exposed to the solution since the presence of the more hydrophobic 2,2'-biphenylpropane moiety in **2** is expected to induce a higher degree of signal blocking in the $\text{Fe}(\text{CN})_6^{3-}$ anion than the more hydrophilic poly(ethylene glycol) chain of **1**. Additionally, examination of molecular models indicates that the monolayer thickness of **2** (38 Å) is higher than that of **1** (29 Å), which could also account for the higher impedance observed (Figure 1).

From the impedance data, the fractional electrode coverages (θ) were calculated using the equation

$$(1 - \theta) = R_{\text{ct}}^0 / R_{\text{ct}}$$

where R_{ct}^0 and R_{ct} are the charge-transfer resistance at the bare and modified electrodes, respectively, with $R_{\text{ct}}^0 = 5 \text{ k}\Omega$. The θ values obtained were 0.940 and 0.989 for **1** and **2**, respectively, indicating the presence of some defects in the monolayer.

It is well-known that thiolated compounds adsorbed on gold surfaces undergo a desorption process at negative potentials in strongly alkaline solution.²⁰ Therefore, SAMs of **1** and **2** were also characterized by reductive desorption experiments by immersing the modified gold electrodes into thoroughly degassed 0.5 M KOH. The scans were initiated at a potential of 0 V and swept cathodically to a potential of -1.2 V at a scan rate of 50 mV/s, exhibiting an irreversible cathodic wave around -1.0 V , which is due to the reductive desorption of the surface-attached thiolate groups (Figure 4). The position of the desorption peaks for **1** and **2** are similar to those previously reported for SAMs of alkanethiols on gold.²⁰ By integrating the current under the

(20) Widrig, C. A.; Chung, C.; Porter, M. D. *J. Electroanal. Chem.* **1991**, 310, 335.

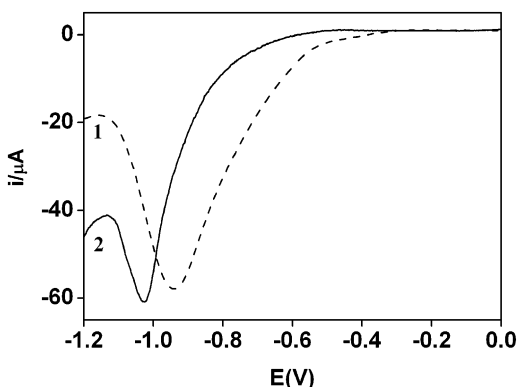


Figure 4. Linear sweep voltammograms (in 0.5 M KOH) for the reductive desorption of **1** (dotted line) and **2** (solid line).

cathodic wave, the estimated surface concentrations were $\Gamma_1 = 2.8 \times 10^{-10}$ and $\Gamma_2 = 1.1 \times 10^{-10}$ mol/cm² assuming the exchange of two electrons during the reduction process. These values translate into molecular surface areas of 59 and 151 Å² for immobilized **1** and **2**, respectively. These differences can be explained considering the higher bulkiness of the chain of **2**, due to the presence of the large *bis*-phenol group, as compared with the linear oligoethyleneglycol chain of **1**. In fact, inspection of molecular models suggest that the molecules of **2** are more separated in a monolayer than in the case of **1**, thus occupying a higher surface area.

Carboxylic acid terminated monolayers should be neutral at low pH due to the protonation of the carboxyl group and develop a negative charge as the pH is raised. This property is relevant in the construction of tunable surfaces that change their characteristics upon variation of an external stimulus. The interfacial acid–base properties of SAMs of dithiol **1** and **2** were studied by recording the CV of Fe(CN)₆^{3−} at different pH (Figure 5). As anticipated, the CV response of Fe(CN)₆^{3−} on SAMs of **1** and **2** strongly depends on the pH of the solution. At acidic pH (pH 1.4), a quasireversible CV signal is observed at the SAM of **1** (Figure 5a) with $E_{1/2} = 0.33$ V and $\Delta E_{ac} = 0.11$ V, indicating that the monolayer of **1** is neutral and blocks to a low extent the electron-transfer process from the anionic Fe(CN)₆^{3−} probe (see a comparison of CV responses at bare and modified electrode in Figure 5a, inset). As the pH of the solution is raised, deprotonation of the COOH groups provokes an increased blocking of the CV signal due to the electrostatic repulsion between the negatively charged surface and the anionic probe. The dependence of cathodic current recorded at 0.39 V as a function of pH showed an inflection point at pH = 4.2, which corresponds to the interfacial pK_a of the SAM of **1** (Figure 5b). Similarly, the potential of the anodic peak is shifted toward less positive values with increasing pH; in this case the pK_a value was estimated to be 3.8. Although the pK_a of **1** in aqueous solution could not be determined due to its low water solubility, the observed values for the interfacial process were found to be 0.6–0.9 units higher than that of 2-methoxyacetic acid ($pK_a = 3.33$), which has a similar structure to the terminal exposed part of the SAM of **1**.²¹ A similar behavior was observed for the SAM of **2**. In this case, the interfacial pK_a was found to be 6.1, about 1.3 units higher than that of propanoic acid ($pK_a = 4.83$).²² This decrease in acidity of COOH groups upon monolayer formation is in agreement with other reports and

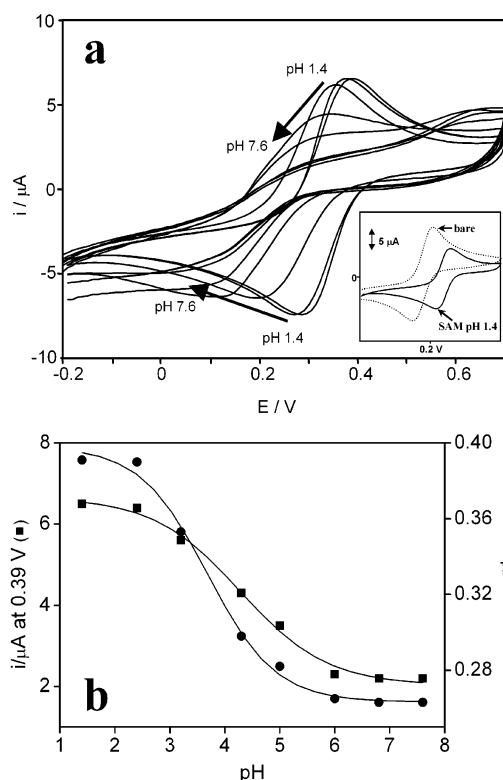


Figure 5. (a) Cyclic voltammograms (in 1 mM K₃Fe(CN)₆ in 0.1 M KCl) obtained at different pH values on a gold electrode modified with **1**. The pH was initially set at 1.4 with HCl and adjusted to the desired value by addition of 0.1–1 M NaOH aliquots. A comparison of CV responses obtained at bare and SAM (pH 1.4) modified electrode is shown in the inset. (b) Titration curves corresponding to the variations of the current intensity at 0.39 V (■) and anodic peak potential (●). The solid lines were obtained by fitting the experimental points to a sigmoidal curve.

results from a combination of electronic, steric and solvent effects.²³ Applications of this property in optimizing protein orientation are currently being studied.

Permeability to electron transfer of the layer carrying the biorecognition entity is a crucial property in the development of electrochemical biosensors as it is related with the sensitivity of the device. To study this property, SAMs of **1** and **2** were prepared and the electrochemical response of *p*-aminophenol (pAP), which undergoes a proton-coupled two-electron oxidation to quinonimine (Figure 6a), was examined. pAP has been widely studied in the development of amperometric biosensors, either as an electron-transfer mediator in peroxidase-catalyzed reactions²⁴ or as the product generated by phosphatase or glycosidase labels.^{16,25} As can be seen, pAP exhibits a quasireversible CV response on both SAMs (Figure 6b), indicating that the electron-transfer process is not blocked by the chemisorbed dithiols. This is in sharp contrast with the suppressed response obtained at a SAM of an aliphatic monothiol, 11-mercaptoundecyl-tetraethyleneglycol (HS(CH₂)₁₁(OCH₂CH₂)₄OH), which has a similar chain length (28 Å) than dithiol **1**. In addition, differential pulse voltammograms of increasing concentrations of pAP (0–10 μM) obtained at a SAM

(22) Serjeant, P.; Dempsey, B. *Ionization Constants of Organic Acids in Aqueous Solution*; Pergamon: Oxford, 1979.

(23) Chechik, V.; Crooks, R. M.; Stirling, C. J. M. *Adv. Mater.* **2000**, *12*, 1161.

(24) Sun, W.; Jiao, K.; Zhang, S.; Zhang, C.; Zhang, Z. *Anal. Chim. Acta* **2001**, *434*, 43.

(21) Richard, J. P.; Williams, K. B. *J. Am. Chem. Soc.* **2007**, *129*, 6952.

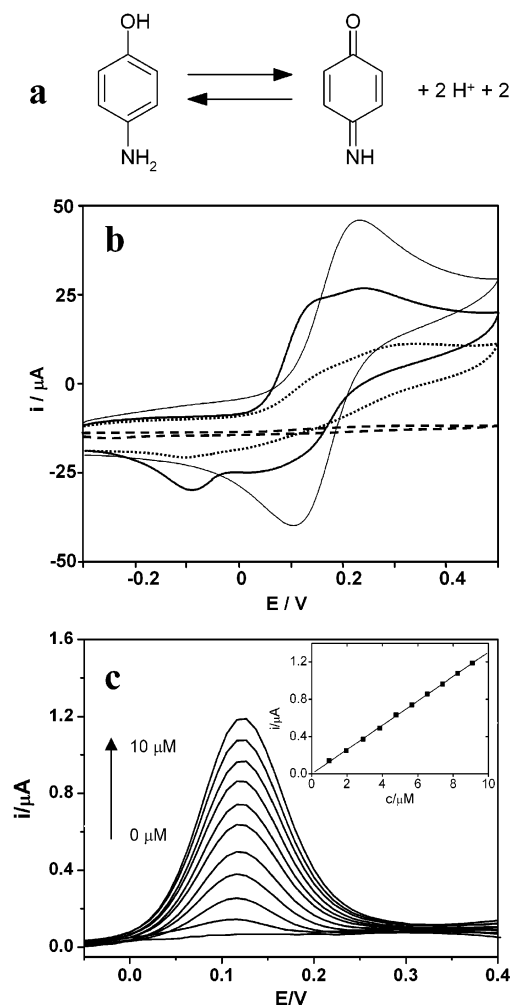


Figure 6. (a) Mechanism of pAP oxidation. (b) Cyclic voltammograms (in 0.1 mM pAP in 0.1 M phosphate buffer pH 7) obtained at bare gold (—) and SAMs of **1** (---), **2** (····), and 11-mercaptoundecyl-tetraethyleneglycol (— · —). (c) DPV response of pAP (0–10 mM in 0.1 M phosphate buffer pH 7) at a SAM of **1**. The i_p vs c calibration plot is showed in the inset.

of **1** revealed that this monolayer is capable of detecting pAP with a low LOD (0.02 μ M), as obtained from the i_p vs c calibration plot (Figure 6c). Therefore, it can be suggested that the disubstitution pattern on positions 3 and 5 of the benzylic core generates some intermolecular “empty” space, allowing for a closer proximity of the electroactive probe to the electrode surface, which is in contrast with the insulating behavior of the aliphatic monothiol (Figure 7).

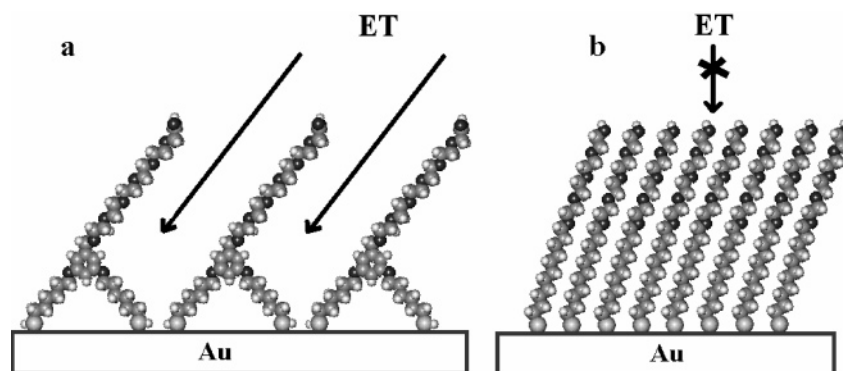


Figure 7. Idealized representation of a SAM of **1** (a) and 11-mercaptoundecyl-tetra(ethylene glycol) (b). ET, electron transfer.

Table 1. Resistance to Charge-Transfer (R_{ct}) Values Obtained at Various Surfaces

surface	analyte	R_{ct} (k Ω)	NSB (%) ^a
Au/ 1		88.1	
Au/ 1	1 μ g/mL PSA	99	12.4
Au/ 2		720	
Au/ 2	1 μ g/mL PSA	895	24.3
Au/ 1 anti-CEA		136	
Au/ 1 anti-CEA	1 μ g/mL PSA	145	6.6
Au/ 1 anti-PSA		71.9	
Au/ 1 anti-PSA	1 μ g/mL CEA	79.8	10.9

^a NSB, $100(R_{ct}^{\text{analyte}} - R_{ct}^{\text{non-analyte}})/R_{ct}^{\text{non-analyte}}$, where NSB is the degree of nonspecific binding and $R_{ct}^{\text{non-analyte}}$ and R_{ct}^{analyte} represent the R_{ct} values before and after incubation of the surface with 1 μ g/mL of the selected analyte.

Dithiol SAMs as supports for antibody immobilization and antigen detection. In immunosensors, the target analyte must be recognized by the immobilized catching antibody (specific binding), while avoiding interaction with the surface (nonspecific binding). Therefore, we evaluated using EIS the occurrence of nonspecific interactions on SAMs of **1** and **2** (in which the carboxyl groups have been modified with ethanolamine) as well as modified SAMs carrying specific and nonspecific antibodies toward PSA, using another tumor marker, the carcinoembryonic antigen (CEA) as nonspecific analyte (Table 1, Figure 8a). The degree of nonspecific binding was calculated by dividing the variation in R_{ct} of the electroactive marker upon analyte binding by the R_{ct} value obtained before analyte interaction (see Table 1). Initially, impedance measurements showed the occurrence of a relatively high degree (>20%) of nonspecific adsorption on a SAM of **2** as compared with **1** (12%) when they are exposed to 1 μ g/mL of PSA. For this reason, dithiol **2** was not subsequently used in these preliminary studies. The degree of nonspecific interactions of **1** toward PSA was 2-fold reduced (up to 6.6%) when this SAM was modified with a nonspecific antibody (anti-CEA). In addition, since one of the objectives of this work is the impedimetric detection of PSA, anti-PSA was immobilized on a SAM of **1** and incubated with 1 μ g/mL of CEA as a nonspecific antigen. In this case, the R_{ct} increased in 10.9%, which could be a consequence of the higher molecular weight and structural complexity of CEA (a 200 kDa glycoprotein). Thus, the low degree of nonspecific binding obtained with **1** indicates that this surface is useful in the construction of immunosensors.

Another important aspect in immunosensor development is the optimization of the specific response of antibody-modified surfaces to avoid a possible intermolecular steric hindrance caused by a

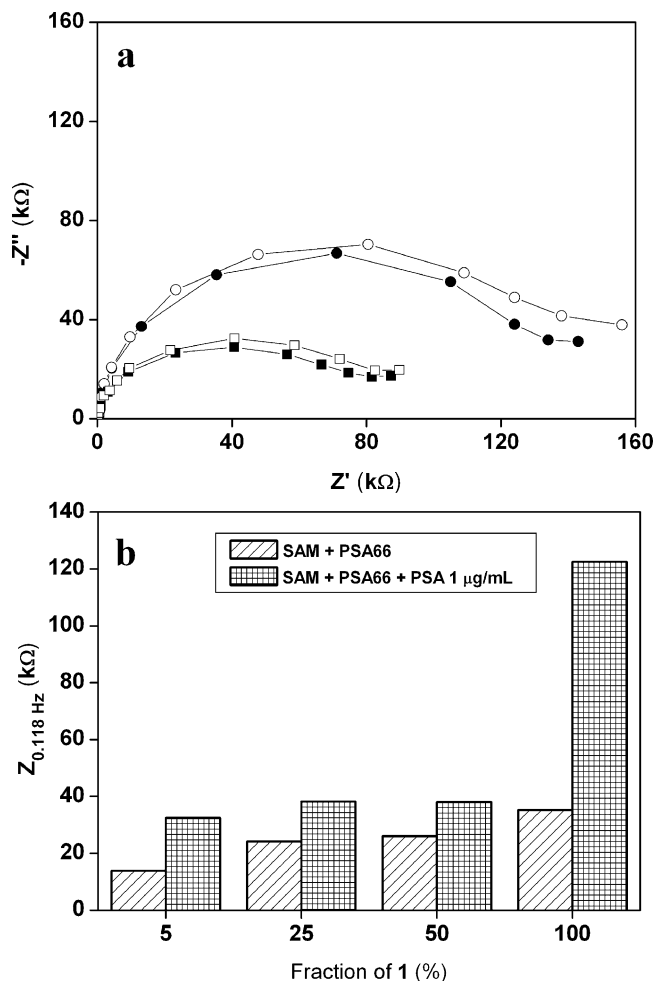


Figure 8. (a) Complex impedance plots (in 1 mM $K_3Fe(CN)_6$ solution in PBS pH 7.4) recorded at a SAM of **1** modified with: anti-PSA (■), anti-PSA in the presence of 1 $\mu\text{g/mL}$ CEA (□), anti-CEA (●), anti-CEA in the presence of 1 $\mu\text{g/mL}$ PSA (○). (b) Total impedance (at 0.118 Hz) for different monolayer compositions in the absence and in the presence of 1 $\mu\text{g/mL}$ PSA antigen.

nonoptimal separation of the immobilized recognition units. For this, gold surfaces were modified with SAMs of different **1**:**3** molar compositions (100:0, 50:50, 25:75 and 5:95) onto which a PSA specific monoclonal antibody (PSA66) was covalently immobilized in order to check if using a mixed SAM to 'space-out' antibodies would lead to a reduction in steric hindrance and an enhanced access of the antigen,^{26,27} as well as **3** contributing to a reduced nonspecific binding. As expected, impedance measurements revealed that there is an increase in the PSA66 immobilization level with increasing proportions of **1** (Figure 8b) due to the increased number of attachment points of the surface. More interestingly, the response of each system to the presence of 1 $\mu\text{g/mL}$ of antigen is markedly higher for the 100% composition with respect to those with lower proportion of **1**. In this SAM, the total impedance after antigen incubation increased by a factor of 3 with respect to the antibody-modified surface. This value is

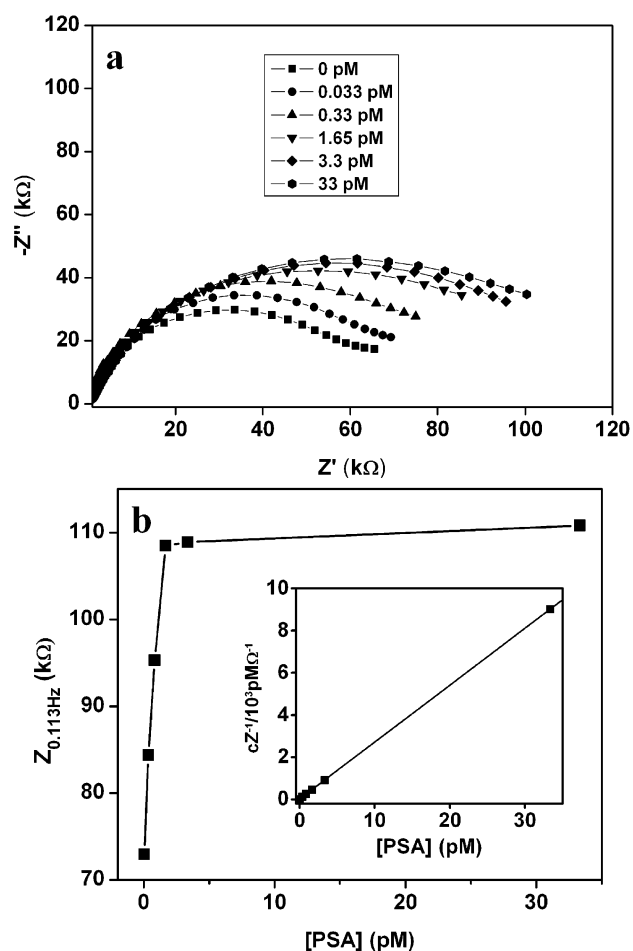


Figure 9. (a) Complex impedance profiles for the detection of PSA antigen (0–33 pM) on a SAM of **1** modified with PSA66 (in 1 mM $K_3Fe(CN)_6$ solution in PBS pH 7.4). (b) Dependence of total impedance (at 0.118 Hz) as a function of PSA concentration. The cZ vs c Langmuir plot is shown in the inset.

only comparable with the 2.2-fold increase observed at the SAM with 5% of **1**. However, the monolayer of 100% of **1** exhibited highest absolute impedance variation, indicating an optimal antigen binding for this composition. This observation differs from previous reports in which mixed SAMs with low carboxylate group contents exhibited the maximum sensing performance.^{26,27} Therefore, we can postulate that the structure of a pure monolayer of **1**, in which the attachment points (COOH groups) are more separated from each other than in the case of a SAM of aliphatic chain monothiol, is sufficient to allow an optimal spacing and orientation of the linked antibodies for maximal binding, at least for the model system under study. This represents an advantage of **1** over previous approaches since one-component SAMs are easier to prepare and their structure is more reproducible and controllable than mixed SAMs.

PSA antigen was impedimetrically detected at 24 °C in a labelless assay by a SAM of **1** modified with anti-PSA antibody by recording the EIS spectra of the antibody modified SAM in the presence of increasing concentrations of PSA (Figure 9a). The signal tends to saturation for concentrations above 100 ng/mL (3.3 pM) of PSA, as expected for the interaction of a solution analyte with an immobilized catching probe (Figure 9b). The data was thus interpreted in terms of the Langmuir isotherm according to the equation

- (25) Masson, M.; Liu, Z.; Haruyama, T.; Kobatake, E.; Ikariyama, Y.; Aizawa, M. *Anal. Chim. Acta* **1995**, *304*, 353.
 (26) Frederix, F.; Bonroy, K.; Laureyn, W.; Reekmans, G.; Campitelli, A.; Dehaen, W.; Maes, G. *Langmuir* **2003**, *19*, 4351.
 (27) Huang, L.; Reekmans, G.; Saerens, D.; Friedt, J.-M.; Frederix, F.; Francis, L.; Muyldermans, S.; Campitelli, A.; Van Hoof, C. *Biosens. Bioelectron.* **2005**, *21*, 483.

$$\frac{c}{Z} = \frac{1}{KZ_{\max}} + \frac{c}{Z_{\max}}$$

where c is the antigen concentration, Z is the impedance at a given concentration, Z_{\max} is the saturation impedance and K is the equilibrium (association) constant. Linear regression of the c/Z vs c plot (Figure 9b, inset) afforded $Z_{\max} = 170 \text{ k}\Omega$ and $K = 13.5 \text{ pM}^{-1} = 1.35 \times 10^{-11} \text{ M}^{-1}$. This value of the affinity constant is in excellent agreement with previous reports,²⁸ demonstrating that the high affinity of the immobilized antibody remains unaltered. Assuming a linear behavior between 0 and 50 ng/mL (0–1.6 pM), the sensitivity of the assay was $706 \text{ k}\Omega \cdot \text{mL} \cdot \text{ng}^{-1}$ and the detection limit was 9 ng/mL (0.3 pM). This value is inside the commonly accepted concentration range used in the clinical diagnosis of prostate cancer (4–10 ng/mL) and agrees well with previous reports on the impedimetric detection of PSA.^{17,18}

CONCLUSIONS

As we have shown, dithiol modified surfaces can be prepared in relatively short periods of time as compared with other

alkanethiol SAMs which in many cases require at least an overnight period of interaction. These SAMs are also stable, permeable to electron transfer, possess low nonspecific binding properties and provide an adequate spacing of the biorecognition molecules. The high antigen–antibody association constant and low detection limit obtained in the labelless detection of PSA strongly support the feasibility of the use of these single dithiol-modified surfaces as supports for recognition elements in biosensors. Further applications of these SAMs in amperometric biosensors are currently being studied.

ACKNOWLEDGMENT

This work has been carried out with financial support from the Commission of the European Communities, RTD programme 'Smart Integrated Biodiagnostic Systems for Healthcare, Smart-HEALTH, FP6-2004-IST-NMP-2-016817'. The authors thank Fujirebio Diagnostics AB for providing the monoclonal antibodies. A.F. thanks Ministerio de Ciencia y Tecnología, Spain, for a "Ramón y Cajal" Research Professorship.

Received for review October 24, 2007. Accepted January 31, 2008.

AC702195V

(28) Paus, E.; Nustad, K.; Børner, O. P. *Tumor Biol.* **1999**, *20*, 52.